Original Research Article

Nuclear Structure of Ce nuclei within Interacting Boson Model-2

Abstract

Using the Interacting Boson Model-2 (IBM-2), we determined the most appropriate Hamiltonian for the current calculations of energy levels and electromagnetic transition probability values of $^{124\text{-}138}$Ce nuclei with a mass around $A = 140$ in this study. We estimated energy levels and electromagnetic values and mixing ratios $\delta(E2/M1)$ for a number of transitions in $^{124\text{-}138}$Ce isotopes using the best fitted values of parameters in the IBM-2 Hamiltonian. When the results were compared to the experimental data, they were found to be in good agreement.

Key Words: Interacting Boson Model-2 (IBM-2), Energy Spectra, Electromagnetic Transitions and Mixing Ratios.

Introduction

The nucleus ground-state and transition charge densities serve as a common foundation for theory and experiment. Nuclei with a neutron number of $N = 82$ and partial proton shell closure of $Z = 58$ make for interesting electron scattering scenarios for studying specific features of nuclear structure. The multipolarities of interband transitions in cerium nuclei are poorly understood. Husar *et al*., **[1]** and Nolan *et al*., **[2]** acquired both energy level spacing and life-time data on ^{130,132,134}Ce in previous investigations, indicating greater collective behavior with decreasing neutron number. Saladin *et al*., **[3]** investigated evidence for continuum E0 transitions following the decay of high-spin states in ^{130}Ce isotope, while Wells *et al*., **[4]** uncovered evidence for collective behavior in ^{128}Ce isotope through lifetime measurements. There has been no extensive work on the structure of cerium nuclei hence calculations that are equivalent to experimental data are required. One of the objectives of this research is to compare prior experimental and theoretical results with interacting boson model predictions in the mass area of $A = 140$.

The Interacting Boson Model (IBM) is based on general algebraic group theoretical approaches that have lately found use in atomic, molecular, and high-energy physics **[5,6]**. It provides a basic Hamiltonian capable of characterizing collective nuclear properties across a wide range of nuclei.

When the first version of the Interacting Boson Model-1 (IBM-1) **[7]** is employed, no distinction is made between proton and neutron variables, and it has been frequently utilized for explaining the quadrupole collective states of medium heavy nuclei. As a result, the incorporation of cubic terms in the boson operators can be used to express triaxiality directly. However, the microscopic foundations clearly say that explicitly describing the proton and neutron variables is critical. This is also a generalized definition of the Interacting Boson Model a second model edition (IBM-2 model). When the first version of the model (IBM-1) is employed, no distinction is made between proton and neutron variables, and it has been frequently utilized for

explaining the quadrupole collective states of medium heavy nuclei. As a result, the incorporation of cubic terms in the boson operators can be used to express triaxiality directly. However, the microscopic foundations clearly say that explicitly describing the proton and neutron variables is critical. This is also a generalized definition of the IBM-2 second version. The s_π, s_ν and d_π, d_ν-bosons, which are approximations to proton (neutron) pairs with angular momentum-parity 0^+ and 2^+, are the building blocks of IBM-2. The fermion operators' boson images are described in terms of the OAI (Otsuka, Arima and Iachello) mapping **[7]**. The extraordinarily strong neutron–proton interaction has been hypothesized as a cause of alterations in nuclei structure. It's also been hypothesized that the neutron–proton effective interactions have a tendency to cause deformation, whereas the neutron–neutron and proton–proton interactions are spheriphying **[8,9]**. A considerable number of nuclei in the medium-heavy and heavy nuclei display features that are neither anharmonic quadrupole vibrational spectra nor distorted rotors. When expressing such nuclei in a geometric description, the typical description of these processes has been given in terms of nuclear triaxiality, which goes from rigid triaxial shapes to softer potential energy surfaces. IBM Hamiltonian takes different forms depending on the regions ($SU(5), SU(3)$ and $O(6)$) of the traditional IBM triangle.

This work focused on the structures of $^{124\text{-}138}$Ce isotopes in order to understanding more about neutron-rich isotopes. The goal is to calculate electromagnetic transition probabilities B(E2) and B(M1) of Ce isotopes around the mass region $A = 140$ using the most appropriate IBM-2 Hamiltonian in valence space, as well as to provide a detailed description of their structure in the dynamic symmetry limits.

The Model

The IBM-2 Hamiltonian can be expressed as

$$H = H_\pi + H_\nu + V_{\pi\nu} \ldots\ldots\ldots\ldots\ldots\ldots (1)$$

Where H_π corresponds to the Hamiltonian of the proton bosons and H_ν is the Hamiltonian of neutron bosons, $V_{\pi\nu}$ quantifies the proton-neutron interaction. $H_{\rho=\pi,\nu}$ can be written in a multipole expansion as:

$$H = \varepsilon_\pi n_{d\pi} + \varepsilon_\nu n_{d\nu} + \kappa(Q_\pi . Q_\nu) + V_{\pi\pi} + V_{\nu\nu} + M_{\pi\nu}(\xi_1, \xi_2, \xi_2) \ldots\ldots\ldots (2)$$

The proton (neutron) d-boson number operator is $n_{d\rho}$, and κ is the quadrupole-quadrupole interaction strengths. Q_ρ is quadrupole operator which is given by the form:

$$Q = \left[\left(d^+ \times s^{\sim}\right)^{(2)}_\rho + \left(s^+ \times d^{\sim}\right)^{(2)}_\rho\right] + \chi_\rho \left[d^+ \times d^{\sim}\right]^{(2)}_\rho \ldots\ldots\ldots (3)$$

$V_{\pi\pi}(V_{\nu\nu})$ is the proton-proton interaction and neutron-neutron interaction respectively.

$$V_{\rho\rho} = \sum_{L} L^{\wedge}\left(C_{L\rho}/2\right)\left[\left(d^{+}\times d^{+}\right)^{(L)}_{\rho}\times\left(\tilde{d}\times\tilde{d}\right)^{(L)}_{\rho}\right]^{(0)}_{\rho} \quad \ldots\ldots\ldots (4)$$

The final element, known as the "Majorana force," fixes the position of states with mixed proton-neutron symmetry, such as $[N_\pi, N_\nu - 1,1], [N_\pi, N_\nu - 2,2]$, etc., and so on, in relation to fully symmetric states.

$$M_{\pi\nu}(\xi_1,\xi_2,\xi_3) = \xi_2\left[\left(d^{+}_{\pi}s^{+}_{\nu} - s^{\sim}_{\pi}d^{\sim}_{\nu}\right)^{(2)}(d^{\sim}_{\pi}s^{\sim}_{\nu} - s^{\sim}_{\pi}d^{\sim}_{\nu})^{(2)}\right]^{(0)} - 2\sum_{k=1,3}\xi_k\left[(d^{+}_{\nu}d^{+}_{\pi})^{(k)}(d^{\sim}_{\nu}d^{\sim}_{\pi})^{(k)}\right]^{(0)} \ldots\ldots (5)$$

For a simplicity we use $\varepsilon_s = \varepsilon_d = \varepsilon$.

Results and Discussion

1- Interaction Parameters

As a result of our calculations, we determine that the four parameters $\varepsilon, \kappa, \chi_\pi$ and χ_ν, essentially entirely define the structure of the spectra. In general, these quantities may be affected by the amount of proton bosons (N_π) and neutron bosons (N_ν). Using **ref.[5]** microscopic calculations as a guide. We have assumed that only ε and κ depend on N_π, and N_ν,i.e., $\varepsilon(N_\pi, N_\nu)$, $\kappa(N_\pi, N_\nu)$, while χ_π depends only on N_π and χ_ν depend on N_ν, i.e., $\chi_\pi(N_\pi)$, $\chi_\nu(N_\nu)$. As a result, a set of isotopes (constant N_π) have the same χ_π value, whereas a set of isotones (constant N_ν) have the same χ_ν value. This parametrization allows a vast number of experimental data to be correlated. When a proton-proton $V_{\pi\pi}$, and neutron-neutron, $V_{\nu\nu}$ interaction is introduced, the coefficients C_L are taken as $C^{\nu}_{L}(N_\nu)$ and $C^{\pi}_{L}(N_\pi)$, respectively, implying that the proton-proton interaction will only be affected by N_π, and the neutron-neutron interaction will only be affected by N_ν (see Table (1)).

Table (1): IBM-2 Hamiltonian Interaction Parameters for Ce isotopes in MeV units except the parameters χ_π and χ_ν are dimensionless

Parameters	^{124}Ce	^{126}Ce	^{128}Ce	^{130}Ce	^{132}Ce	^{134}Ce	^{136}Ce	^{138}Ce
ε	0.060	0.175	0.255	0.400	0. 503	0.675	0.685	0.951
κ	-0.197	-0.220	-0.215	-0.230	-0.225	-0.230	-0.198	-0.122
χ_ν	-0.675	-0.450	-0.250	-0.206	-0.090	-0.080	-0.075	-0.065
χ_π	-0.415	-0.295	-0.155	-0.175	-0.080	-0.080	-0.075	-0.065
ξ_2	0.05	0.05	0.05	0.12	0.12	0.10	0.10	0.10
$C_{2\nu}$	-0.015	-0.015	-0.015	-0.03	-0.03	-0.04	-0.03	-0.03
$C_{4\nu}$	0.03	0.03	0.03	0.03	0.03	0.04	0.03	0.03

$\xi_1 = \xi_3 = 0.02$ MeV, $C_{0\pi} = C_{2\pi} = C_{4\pi} = 0$ MeV , $C_{0\nu} = 0$ MeV

The following is a summary of the approach we used to determine the parameters: To acquire the best fit for the Ce isotopes, the parameters ε and κ must first be found while retaining $C_{0\pi} = C_{2\pi} = C_{4\pi} = 0$ MeV, $C_{0\nu} = 0$ MeV.

2-Energy Spectra

The energy spectra of the Ce isotopic chains in the major shell 50-82 were calculated using the IBM-2 Model is presented. Figure (l), show the results. The Figure (1) show a detailed comparison with experiment, where states have been divided into three groups to make the comparison more evident. Table (1) shows the resultant parameters. They are the finest simultaneous fits for the entire region that we have. It should be noted that these graph include calculations for nuclei that are currently unknown. Combining the results of this study with comparable estimates for the isotope chains Ru and Pd **[10]** yielded the parameters for these unknown locations.

The energy ratios $R = E(4_1^+)/E(2_1^+)$ it is clear that the ratio decreases from its highest value at the isotope ^{124}Ce ($R = 3.168$) smoothly to the lowest value at the isotope ^{136}Ce ($R = 2.316$). Thus, these isotopes take the transitional symmetry, that is, they fall within the O(6) limit.

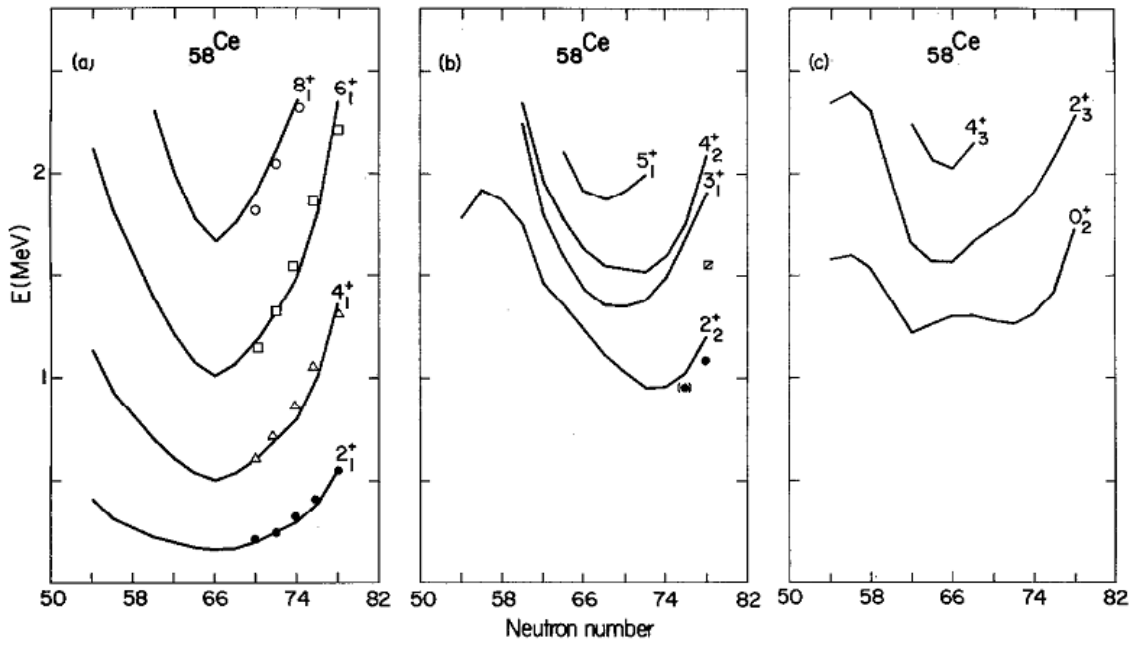

Figure (1): Comparison between calculated and experimental energy levels in Ce. The experimental levels are taken from refs. [11-18].

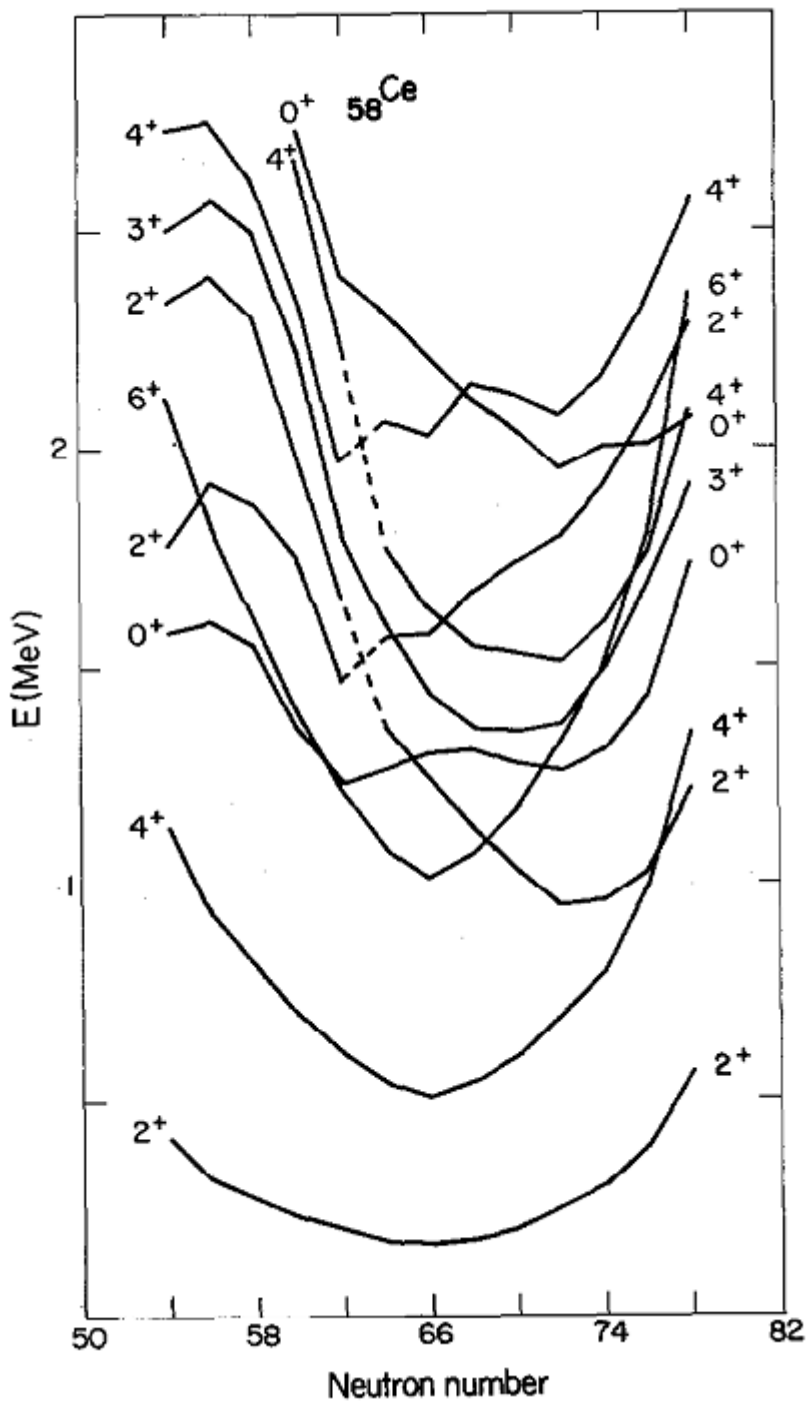

Figure (2): IBM-2 Calculation energy spectra in the Ce isotopes, note that between neutron number 62 and 64 the third and second 2^+ and 4^+ states exchange their electromagnetic properties.

3- Electric Transition Probability

After the wave functions have been determined by fitting the energy levels, all additional nuclear properties can be calculated. We'll start with electromagnetic transition rates. The E2 boson operator is defined as follows:

$$T^{(E2)} = T_{\pi}^{(E2)} + T_{\nu}^{(E2)} \quad \text{..... (6)}$$

Where

$$T_{\rho}^{(E2)} = e_{\pi} Q_{\pi} + e_{\nu} Q_{\nu} \quad \text{..... (7)}$$

The reduced electric quadrupole transition probability between states is written as:

$$B(E2; J_i^+ \rightarrow J_f^+) = \frac{1}{2J_i + 1} \left| < J_f^+ \left\| T^{(E2)} \right\| J_i^+ > \right|^2 \text{..... (8)}$$

In principle, the operator Q_{ρ} could be different from the Hamiltonian's operator (3). We've assumed it's the same for the sake of simplicity. The boson effective charges e_{π} and e_{ν} is then the only factors that affect electromagnetic transition rates.

On the same microscopic basis [5,] we expect e_{π} to be solely dependent on N_{π} and e_{ν} to be solely dependent on N_{ν}. We've retained the effective charges normalized to the experimental values of $B(E2; 2_1^+ \rightarrow 0_1^+)$ to get $e_{\pi} = e_{\nu} = 0.124$ *e.b* for all nuclei because we're only interested in primary features at this point.

Our results for the $B(E2; 2_1^+ \rightarrow 0_1^+)$ values are shown in Table (2). It's worth noting how the $B(E2)$ values improve as you go closer to the middle of the shell. Our results for the $B(E2; 2_2^+ \rightarrow 2_1^+)$ values are displayed in Table (2). There is a scarcity of experimental data on this quantity. Finally, we show the findings for $B(E2; 2_2^+ \rightarrow 0_1^+)$ values, because this transition is forbidden in all three limits of the interacting boson model, this amount is quite small.

Table (2): Electric Transition Probability in $e^2.b^2$ for Ce Isotopes

Isotopes	Transitions	Exp. [11-18]	IBM-2
^{124}Ce	$2_1^+ \rightarrow 0_1^+$	-	0.887
	$2_2^+ \rightarrow 2_1^+$	-	0.0275
	$2_2^+ \rightarrow 0_1^+$	-	0.0330
	$4_1^+ \rightarrow 2_1^+$	-	1.2559
^{126}Ce	$2_1^+ \rightarrow 0_1^+$	0.5178 (24)	0.695
	$2_2^+ \rightarrow 2_1^+$	-	0.058
	$2_2^+ \rightarrow 0_1^+$	-	0.042
	$4_1^+ \rightarrow 2_1^+$	0.6941(17)	0.748
^{128}Ce	$2_1^+ \rightarrow 0_1^+$	0.4253 (12)	0.444
	$2_2^+ \rightarrow 2_1^+$	-	0.193
	$2_2^+ \rightarrow 0_1^+$	-	0.039
	$4_1^+ \rightarrow 2_1^+$	0.6897 (4)	0.782
^{130}Ce	$2_1^+ \rightarrow 0_1^+$	0.3482 (4)	0.448
	$2_2^+ \rightarrow 2_1^+$	-	0.259
	$2_2^+ \rightarrow 0_1^+$	-	0.023
	$4_1^+ \rightarrow 2_1^+$	0.6533 (20)	0.633
^{132}Ce	$2_1^+ \rightarrow 0_1^+$	0.3713 (7)	0.359
	$2_2^+ \rightarrow 2_1^+$	-	0.427
	$2_2^+ \rightarrow 0_1^+$	-	0.004
	$4_1^+ \rightarrow 2_1^+$	0.4112 (23)	0.492
^{134}Ce	$2_1^+ \rightarrow 0_1^+$	0.2118 (5)	0.268
	$2_2^+ \rightarrow 2_1^+$	-	0.343
	$2_2^+ \rightarrow 0_1^+$	-	0.001
	$4_1^+ \rightarrow 2_1^+$	0.1589 (8)	0.263
^{136}Ce	$2_1^+ \rightarrow 0_1^+$	0.1620 (5)	0.165
	$2_2^+ \rightarrow 2_1^+$	0.1953 (8)	0.239
	$2_2^+ \rightarrow 0_1^+$	0.0022 (9)	0.002
	$4_1^+ \rightarrow 2_1^+$	0.2326 (10)	0.2414
^{138}Ce	$2_1^+ \rightarrow 0_1^+$	0.0898^{+16}_{-14}	0.09758
	$2_2^+ \rightarrow 2_1^+$	0.0001(11)	0.0001
	$2_2^+ \rightarrow 0_1^+$	0.0049 (4)	0.0038
	$4_1^+ \rightarrow 2_1^+$	> 0.012	0.0130

4- Magnetic Transition Probability

In the IBM-2, multipole transition operators have the form that is an extension of the IBM-1 operators. The magnetic transition operators are given by:

$$T^{(M1)} = \sqrt{\frac{3}{4\pi}}\left(g_\pi L^{\wedge}_\pi + g_\nu L^{\wedge}_\pi\right) \ldots\ldots\ldots\ldots\ldots\ldots (9)$$

The g_ρ is the gyromagnetic ratio (g-factors) usually set to $g_\pi = 1\ \mu_N$ and $g_\nu = 0\ \mu_N$. The reduced electric quadrupole transition probability between states is written as:

$$B(M1; J_i^+ \to J_f^+) = \frac{1}{2J_i + 1}\left| < J_f^+ \left\| T^{(M1)} \right\| J_i^+ > \right|^2 \ldots\ldots\ldots\ldots\ldots\ldots (10)$$

The IBM-2 calculations for the magnetic transition probability $B(M1)$ are shows in **Table (3),** from these results; we observe that the transitions between low-lying collective states (symmetric states) are weak. This is because; the anti-symmetric component in the wave functions introduced by *F-spin* breaking in the Hamiltonian is increased. The magnitude of $B(M1)$ values increases with increasing spin for the transitions from $\gamma-$band to gs-band ($\gamma \to g$) and the transitions from gamma to gamma band ($\gamma \to \gamma$).

The IBM-2 predicts a small M1 component, this is due to; the symmetry and forbiddances of gamma band crossing transitions. The size of $\gamma \to g$ M1 matrix elements is decrease with increasing isotopic mass (increasing neutron number), specially, a change in $B(M1)$ strengths for the transition $\gamma \to g$ occurs when the gamma band crossing the beta band (band crossing or band mixing). Unfortunately, the experimental data on M1 transition probability are very rare and also the approximate nature of theory does not make it possible to settle the question of nuclear nonaxiality.

Table (3): Magnetic Transition Probability for $^{124\text{-}138}$Ce isotopes in μ_N^2 units

Isotopes	$2_2^+ \to 2_1^+$	$2_3^+ \to 2_1^+$	$2_3^+ \to 2_2^+$	$3_1^+ \to 2_1^+$
Ce-124	0.00008	0.00046	0.00014	0.00049
Ce-126	0.00003	0.00533	0.00025	0.0043
Ce-128	0.00004	0.00246	0.00076	0.0023
Ce-130	0.0005	0.0034	0.0008	0.0025
Ce-132	0.00001	0.0596	0.0011	0.009
Ce-134	0.00001	0.0480	0.0029	0.0088
Ce-136	0.0019	0.02264	0.031	0.0020
Ce-138	0.0552	0.029	0.0044	0.0092

5-Mixing Ratio $\delta(E2/M1)$

The reduced matrix element ratio $\Delta(E2/M1)$ is directly related to the usual multipole amplitude mixing ratio δ by the expression **[19]**:

$$\delta = 0.835 E_{\gamma}(MeV)\Delta(eb/\mu_N) \quad \text{.....(11)}$$

$$\Delta(E2/M1) = < J_f^+ \| T^{(E2)} \| J_i^+ > / < J_f^+ \| T^{(M1)} \| J_i^+ > \quad \text{..... (12)}$$

The mixing ratios $\delta(E2/M1)$ for $^{124\text{-}138}$Ce isotopes are presented, we depending on the Eq.(11) to evaluate the mixing ratios. The IBM-2 calculations for mixing ratios and the experimental data are tabulated in **Table (4)**. The agreement between IBM-2 values and experimental data is good.

From these results, we can be observed the change in the sign appears in both the $\delta(E2/M1;2_2^+ \to 2_1^+)$ and $\delta(E2/M1;2_3^+ \to 2_1^+)$ in $^{124\text{-}138}$Ce isotope; this is due to, the magnitude for E2 and M1 matrix elements. Moreover, in some isotopes there is an opposite sign between the $\delta(E2/M1;2_2^+ \to 2_1^+)$ mixing ratio and the $\delta(E2/M1;3_1^+ \to 2_1^+)$ mixing ratio, this is because, the differences between states 2_2^+ (symmetric state and it's a member of beta band) and 3_1^+ (mixed symmetry state and it's a member of gamma band).

The large values for some mixing ratios such as $\delta(E2/M1;2_2^+ \to 2_1^+)$ are due to the very small component M1 effect in the transition and a dominant E2 transition. Moreover, IBM-2 found the large value for mixing ratios such as $\delta(E2/M1;2_2^+ \to 2_1^+)$ in Ce isotopes, the compared with experimental value may be related to high predicted the IBM-2 energy level 2_2^+ value. The mixing ratio sign is chosen according to the sign of reduced matrix elements.

Table (4): Mixing Ratios $\delta(E2/M1)$ for $^{124\text{-}138}$Ce isotopes in eb/μ_N units

Isotope	$2_2^+ \to 2_1^+$		$2_3^+ \to 2_1^+$		$3_1^+ \to 2_1^+$		$3_1^+ \to 2_2^+$	
	Exp.	**IBM-2**	**Exp.**	**IBM-2**	**Exp.**	**IBM-2**	**Exp.**	**IBM-2**
^{124}Ce	-	-2.018	-	-0.1776	-	-2.703	-	-2.431
^{126}Ce	-	-4.151	-	0.147	-	-4.930	-	-3.548
^{128}Ce	-	11.47	-	0.0782	4.2^{+24}_{-15}	4.880	-	-8.716
^{130}Ce		14.887	-	0.0848	-	6.805	-	-1.843
^{132}Ce	9^{+15}_{-3}	8.988	-1.4(2)	-0.1330	4.8(6)	5.181	13.2(14)	14.77
^{134}Ce	-	9.627	-	0.0049	-	4.835	-	8.249
^{136}Ce	- 4.7 (7)	-4.624	0.46(8)	0.381	-	0.843	- 4.3 (6)	-5.556
^{138}Ce	-	0.0107	-	0.793	-	4.267	-	1.652

Experimental data are taken from ref. [19].

Concluding Remarks

A complete set of calculations for the Ce isotope chains in the main shell 50-82 is offered here. These calculations show that entire areas of the periodic table can be correlated in a relatively easy manner. We have fitted the properties of certain known nuclei with our calculations, but most crucially, we have predicted a vast number of features in nuclei that are currently unknown. Some of these properties will be evaluated in the near future, thanks to the development of new experimental techniques and facilities. It will be fascinating to see if our predictions match the results of the experiment.

References

[1] D. Husar, S. J. Mills, H. Graf, U. Neumann, D. Pelte and G. Seiler-Clark, Nucl. Phys. **A292** (1977) 267

[2] P. J. Nolan, D. M. Todd, P. J. Smith, D. J. G. Love, P. J. Twin, O. Andersen, J. D. Garrett, G. B. Hagemann and B. Herskind, *Phys. Lett.* **B108**, (1982) 269.

[3] J. C. Wells, N. R. Johnson, J. Hattula, M. P. Fewell, D. R. Haenni, I. Y. Lee, F. K McGowan, J. W. Johnson and L. L. Riedinger, Phys. Rev. **C30**, (1984) 1532.

[4] J. X. Saladin, M. P. Metlay, D. F. Winchell, M. S. Kaplan, I. Y. Lee, C Baktash, M. L. Halbert, N. R. Johnson and O. Dietzsch, *Phys. Rev.* **C53**, (1996) 652.

[5] O. S. Van Roosmalen, A. E. L. Dieperink and F. Iachello, Chem. Phys. Lett. **85**, 32 (1982)

[6] M. E. Kellman and P. R. Herrick, *Phys. Rev.* **A22**, (1980) 1536.

[7] T. Otsuka, A. Arima and F. Iachello, *Nucl. Phys.* **A309**, (1979) 1.

[8] P. Federman and S. Pittel, *Phys. Lett.* **B69**, (1977) 385.

[9] C. K. Nair, A. Ansari and L. Satpathy, *Phys. Lett.* **B71**, (1977) 257.

[10] P. van lsacker and G. Puddu, Nucl. Phys. A348 (1980) 125.

[11] J. Katakura and Z. D.Wu, Nuclear Data Sheets 109 (2008) 1866.

[12] J. Katakura and K. Kito, Nuclear Data Sheets 97 (2002) 866.

[13] M. Kanbe and K. Kito, Nuclear Data Sheets 94 (2001) 368.

[14] Balraj Singh, Nuclear Data Sheets 93 (2001) 184.

[15] Yu. Khazow, A. A. Rodionov, S. Sakharov and Balraj Singh, Nuclear Data Sheets 104 (2005) 687.

[16] A. A. Sonzogni, Nuclear Data Sheets 103 (2004) 112.

[17] A. A. Sonzogni, Nuclear Data Sheets 98 (2003) 910.

[18] N. Nica**,** Nuclear Data Sheets 108 (2007) 584.

[19] J. Lang, K. Kumar and J. H. Hamilton, Rev. Mod. Phys. Vol.54 No. 1 (1982).